phys. stat. sol. (a) **200**, No. 2, 439–445 (2003) / **DOI** 10.1002/pssa.200306702

Optical studies of the Holmium-doped InGaAsP epilayers

Y. C. Lee[1], **G. W. Shu**[1], **I. M. Cheng**[1], **C. P. Chen**[1], **J. L. Shen**[*, 1], **W. Y. Uen**[2], **C. W. Chang**[3], **Y. F. Chen**[3], and **W. C. Chou**[4]

[1] Physics Department, Chung Yuan Christian University, Chung-Li, Taiwan, R.O.C.
Center for Nanotechnology, Chung Yuan Christian University, Chung-Li, Taiwan, R.O.C.
[2] Electronic Engineering Department, Chung Yuan Christian University, Chung-Li,Taiwan, R.O.C.
[3] Physics Department, National Taiwan University, Taipei, Taiwan, R.O.C.
[4] Electrophysics Department, National Chiao-Tung University, Hsin-Chu, Taiwan, R.O.C.

Received 25 August 2003, revised 22 September 2003, accepted 29 September 2003
Published online 4 December 2003

PACS 78.20.Jq, 78.30.Fs, 78.40.Fy, 78.55.Cr

Photoluminescence (PL), contactless electroreflectance (CER), and Raman scattering measurements have been used to study the structural properties of Ho-doped InGaAsP epilayers. Both the full width at half maximum (FWHM) of PL and the broadening parameter of CER are decreased as the doping amount of Ho element increases. This indicates that Ho doping greatly reduces the residual impurities and improve the quality of epilayers. The Raman spectra of Ho-doped InGaAsP epilayers are found to have asymmetric line shapes. Using a spatial correlation model, it is found the asymmetric broadening of the Raman signal is not influenced by the Ho doping. We hence conclude that the introduction of the Ho element can greatly reduce the residual impurities of LPE-grown layers, but no large amounts of Ho element are being incorporated into the epilayers during the purification.

1 Introduction

Recently, doping of III–V compound semiconductors with rare-earth elements is a field of great interest due to its potential application in optoelectronic devices [1–7]. The intracenter transitions of 4f shells of rare-earth elements give rise to sharp luminescence, which would play an active role in the emission devices. A major advantage of the rare-earth doping in III–V semiconductors is that the 4f emission is independent of the band-gap energy of the host crystal, so that its emission wavelength is insensitive to the crystal field and temperature. In addition, the rare-earth elements can act as getting agents to significantly reduce the residual impurities and increase the carrier mobility in the liquid phase epitaxy (LPE) growth [3–7]. During LPE growth, the rare-earth elements form stable compounds with residual impurities caused by chemical reactions, leading to the purification of the semiconductor layers. To date, most studies on this method of purification have focused on the gettering ability of impurities due to the presence of rare-earth elements [3–7]. The effects of rare-earth doping on the fundamental properties of the semiconductors are, to our knowledge, rather limited. An understanding of the fundamental properties of the rare-earth-doped semiconductors is important not only for improving the crystal growth but also extending its application to electronic and optical devices.

One interesting topic regarding the purification with rare-earth doping is whether the rare-earth elements are incorporated into the epilayers during purification [8]. The incorporation of the rare earth elements into the semiconductor epilayers has been demonstrated [9–11]. However, recent studies reported that the resultant compound, which consist of rare-earth elements and impurities are insoluble in the

[*] Corresponding author: e-mail: jlshen@phys.cycu.edu.tw

liquid phase and do not enter into the solid phase after purification; i.e., the rare-earth elements are not incorporated into the host lattice after the rare-earth-doping [12–14]. Raman spectrum provides an effective way to resolve this problem. If the resultant compounds are captured by the solid phase, the grown epilayers should generate stress or produce potential fluctuation. The stress in the grown layers can be detected from the Raman shift, while the potential fluctuations due to imperfections can relax the Raman selection rule, leading to the broadening and asymmetry of the Raman line shape [15]. Therefore, Raman scattering can be an effective technique to investigate the microscopic variation of the rare-earth doped semiconductors.

In this work, we present the influence of Ho doping on the structural properties of quaternary InGaAsP layers using photoluminescence (PL), contactless electroreflectance (CER), and Raman scattering. According to the reduction of the full width at half maximum (FWHM) of PL peak and the broadening parameter of CER, the concentration of residual impurities are found to decrease greatly in the Ho-doped InGaAsP epilayers. Based on a spatial correlation model, the line shapes of Raman scattering were analyzed. This result suggests that no large amounts of Ho element are being incorporated into the epilayers during the purification.

2 Experiment

Ho doped InGaAsP layers studied in this work were grown by LPE on (100) orient InP:Fe substrate. After cleaning, the LPE system was heated at 670 ℃ for one hour to homogenize the melt completely. The temperature was then lowered to 650 ℃ at a rate of 0.5 ℃/min for 0.2 hours to grow an InP buffer layer on substrate. Next, the InGaAsP layer was grown at 640 ℃ follow by cooling at 0.3 ℃/min for 15 min. During growth, the system was flushed with purified hydrogen to maintain atmospheric pressure. After growth, the melt was slid away from the substrate and the graphite boat was rapidly cooled to room temperature to avoid thermal damage of the grown layer. Table I lists the amounts of Ho elements doped into the growth solutions.

The samples were mounted on the cold finger of a closed-cycle helium cryostat and characterized by PL and CER. The PL was measured using a focused Ar ion laser as the excitation source and analyzed with a Jobin–Yvon spectrometer. A germanium photodetector was used to read PL signals. Raman measurements were performed at room temperature in the backscattering. The scattered photons were dispersed by spectrometer and detected with a photon-counting system. In the CER measurements, a condenser-like system consisting of a transparent conducting coating on a transparent substrate was used as the front electrode and a metal strip was used as the second electrode. The a.c. modulating voltage of 500 V at 200 Hz is applied between the metal strip and the transparent electrode. The light from a tungsten-halogen lamp was dispersed through a monochromator and focus on the sample. The reflected light was detected by an InGaAs detector.

3 Results and discussion

Figure 1 shows the PL spectra of the InGaAsP epitaxial layers with various amount of Ho doping. The amount of Ho elements is: (a) undoped (b) 0.017 wt% (c) 0.075 wt% (d) 0.110 wt% (e) 0.150 wt%. The PL studies of rare-earth doped InGaAsP epilayer have been studied previously [12, 14, 16]. According to the previous results, the main peak in Fig. 1 can be assigned as the band-to-band transition [12, 14, 16]. Basically, the FWHM of PL in Ho-doped InGaAsP is reduced with increasing the amount of Ho elements. In Fig. 1, we do not find any peak appears in the wavelength range up to 1700 nm; as a result, there is no spectral feature attributed to the intra-4f-subsell transitions of the Ho ions. This indicates that no appreciable amount of Ho element was introduced into the InGaAsP layers. It is noteworthy to point out that the peak energy of the PL changes slightly after the Ho doping, as listed in Table 1. This change may be explained by the formation of microparticles of the Ho compounds, which will cause a smallchange in the solid composition of InGaAsP layers [3, 9]. The compositional change of the InGaAsP layers thus leads to a change of the energy band gap.

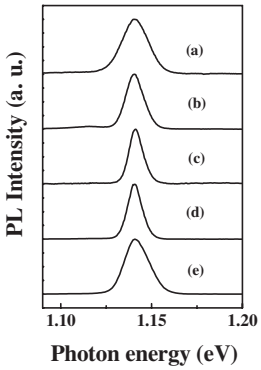

Fig. 1 12 K PL spectra of InGaAsP epilayers as a function of doping amount of the Ho elements: a) undoped b) 0.017 wt% c) 0.075 wt% d) 0.110 wt% e) 0.150 wt%.

The FWHM of PL signals as a function of Ho amount are listed in the Table 1 and shown in Fig. 2. As the amount of Ho element is 0.110 wt% the FWHM has a minimum value of 7.9 meV, which is smaller by about 46% than that of the undoped InGaAsP. Since the FWHM of PL is related to the presence of residual impurities, the narrowing effect due to Ho doping indicates that the Ho doping to InGaAsP layers can greatly reduce the residual impurities and improve the quality of InGaAsP layers. The improvement of sample quality due to rare-earth doping can be further supported by measuring Hall mobility. Table 1 lists the mobility of the InGaAsP epilayers with various amount of Ho doping. We clearly see that the mobility of the InGaAsP epilayers increases with Ho doping. The increased mobility is due to the removal of unwanted impurity and hence the reduction of impurity scattering centers [4, 6]. As the doping amount of Ho element is increased above 0.110 wt%, the FWHM of photoluminescence peak become much broader than that with low amount of Ho doping. This broadening effect could be explained by the fact that too many Ho elements may cause a large lattice mismatch or strain which will result in additional dislocations or defects in the epilayers [12].

Figures 3a–e show the 14 K measured CER spectra (solid curves) from InGaAsP layers with various amount of Ho doping: (a) undoped (b) 0.017 wt% (c) 0.075 wt% (d) 0.110 wt% (e) 0.150 wt%. The CER lineshapes in Fig. 3 display a single feature although there is a change in phase between Fig. 3a and Figs. 3b–e. The phase shift in electroreflectance could be due to the inhomogenous perturbation [17], resulting from the inhomogenous surface electric field influenced by the ionized impurities [18]. Since the undoped InGaAsP layer contains more residual donors (impurities), its CER lineshape can be different from the CER lineshape of Ho-doped InGaAsP layers. These measured CER data were analyzed using the third derivative functional fit (TDFF) model [19], given as:

$$\Delta R/R = \mathrm{Re}\,[C \exp(i\theta)\,(E - E_0 + i\,\Gamma)^{-m}]\,, \tag{1}$$

where E is the incident photon energy, E_0 is the interband transition energy, Γ is the broadening parameter, C and θ are the amplitude and phase, respectively, and m is a number associated with the dimension

Table 1 Values of mobility, PL peak position, PL FWHM, asymmetric ratio of Raman scattering, and correlation length of InGaAsP layers with various amount of Ho elements.

InGaAsP Ho-doped (wt%)	mobility (cm^2/V s)	PL		Raman scattering	
		peak position (eV)	FWHM (meV)	asymmetric ratio (Γ_a/Γ_b)	correlation length L (Å)
undoped	2930	1.1405	14.80	1.68	27
0.017	13962	1.1404	9.87	1.7	25
0.074	14250	1.1411	8.02	1.65	28
0.110	14824	1.1405	7.93	1.68	27
0.150	13344	1.1408	13.02	1.68	27

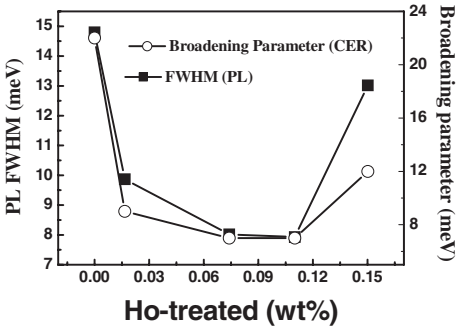

Fig. 2 FWHM of PL and broadening parameter of CER as a function of doping amount of the Ho elements. The solid lines are guides for the eye.

ality of the critical point and is 2.5 for the band-to-band transition of bulk materials. The open circles in Fig. 3 show fits to the TDFF model for a three-dimensional critical point. All the fitting parameters are listed in Table 2. The interband transition energies E_0 in CER are not totally correlated with the peak positions in PL. This could be due to the impurity effects in electroreflectance modulation spectroscopy. Under the applied electric field, several effects, such as impact ionization, back-surface reflection, electro-absorption effect related to the Urbach tail, may affect the interband transition energy in CER [18]. However, the exact origin leading to the discrepancy between PL peak position and E_0 in CER is still not clear. The broadening parameters of the CER spectra shown in Fig. 3 as a function of the amount of Ho are listed and shown in Table 1 and Fig. 2, respectively. Like the PL in Fig. 1, the broadening parameter of CER decreases as the doping amount of Ho element increases. The narrowing effect of the broadening parameter supports our previous argument that the Ho doping can reduces the residual impurities and improve the sample quality.

Incorporation of the rare earth elements into the semiconductor epilayer has also been demonstrated recently [9–11]. However, it has been reported that the rare-earth elements are not incorporated into the host lattice after the rare-earth-doped process; i.e., the LPE melt is doped with rare earth elements, but the grown epilayer is not [12–14]. In order to clarify the purification mechanism using the Ho-doping, the Raman scattering measurements were performed. If the rare-earth compounds, originates from the reaction of the rare-earth elements and impurities, are captured by the epilayers, the grown layers should exhibit a change in their microscopic structure. It is known that the peak position of Raman signal is

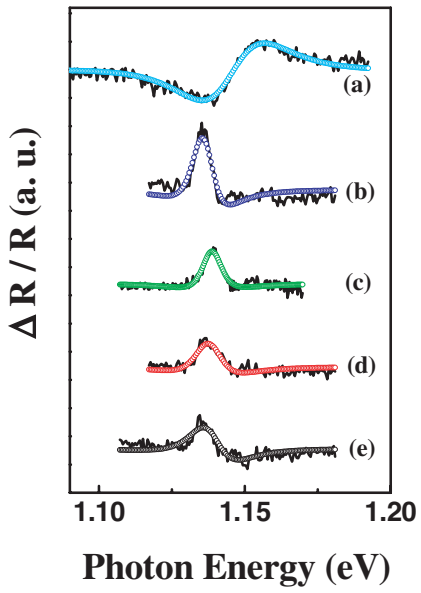

Fig. 3 (online colour at: www.interscience.wiley.com) 14 K CER spectra of InGaAsP epilayers as a function of doping amount of the Ho elements: a) undoped b) 0.017 wt% c) 0.075 wt% d) 0.110 wt% e) 0.150 wt%. The open circles are fits to a TDFF model for a three-dimensional critical point.

Table 2 Values of amplitude, interband transition, broadening parameter, phase, dimensionality in the fitting of CER lineshapes.

InGaAsP Ho-doped (wt%)	C (a.u.)	E_0 (eV)	broadening parameter (meV)	phase θ	m
undoped	3.648×10^5	1.145	22	128.6	2.5
0.017	4.662×10^5	1.138	9	245.0	2.5
0.074	2.659×10^5	1.140	7	223.2	2.5
0.110	2.089×10^5	1.138	10	236.9	2.5
0.150	2.120×10^5	1.141	12	275.3	2.5

related to the stress change, while the lineshape of Raman signal is associated with the structural imperfections [15, 20, 21]. Raman scattering can thus be a powerful technique to investigate the microscopic nature of the Ho-doped epilayers. Figure 4 displays the Raman spectra with various amounts of Ho elements into InGaAsP layer: (a) undoped, (b) 0.017 wt% (c) 0.075 wt% (d) 0.110 (e) 0.150 wt%. The Raman signal peaked at 226 cm^{-1} in Fig. 4 is attributed to the InAs-like LO mode [20–21]. The same peak position of Raman signal in Figs. 4a–e indicates that no strain occurs after Ho doping. The Raman peaks in Fig. 4 have an asymmetric line shape, which can be analyzed by a spatial correlation (SC) model. According to the SC model, the spatial correlation function of the phonon for a pure compound semiconductor is infinite and the phonon eigenstates are plane waves. These lead to the usual $q = 0$ momentum selection rule of Raman scattering and the Raman spectrum shows a symmetric Lorentzian profile ($\Gamma_a = \Gamma_b$, where Γ_a (Γ_b) represents the low-energy (high-energy) half width of half maximum). The alloying or any imperfection in semiconductors may destroy the configurational symmetry and break down the $q = 0$ momentum selection rule. The spatial correlation function of phonon hence become finite and the Raman spectrum reveals an asymmetric line shape ($\Gamma_a > \Gamma_b$). Based on the SC model, we analyze the Raman spectrum in Fig. 4 with a correlation function in a Gaussian form, exp $(-2r^2/L^2)$, where L is the phonon correlation length. The Raman intensity at a frequency ω is given by a Lorentzian function modified by Gaussian distribution: [20, 21]

$$I(\omega) \propto \int \frac{\exp\left(-\frac{q^2 L^2}{4}\right)}{\left[\omega - \omega(q)\right]^2 + \left(\frac{\Gamma_0}{2}\right)^2} d^3q \,, \tag{2}$$

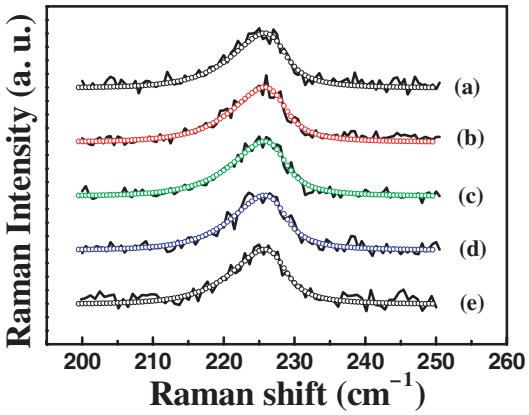

Fig. 4 (online colour at: www.interscience.wiley.com) The Raman spectra of InGaAsP epilayers as a function of doping amount of the Ho elements: a) undoped b) 0.017 wt% c) 0.075 wt% d) 0.110 wt% e) 0.150 wt%.

where q is the reduced wave vector in the unit of $2\pi/a$, a is the lattice constant of InAs, and Γ_0 (=10 cm^{-1} for the InAs-like mode) is the intrinsic linewidth of phonon mode. As for the dispersion $\omega(q)$ of the LO phonon, an analytical formula based on a one-dimensional linear-chain model has been used:

$$\omega^2(q) = A + \sqrt{A^2 - B\{1-\cos(aq)\}}\ , \tag{3}$$

where we take $A = 2.59 \times 10^4\ cm^{-2}$ and $B = 3.58 \times 10^8\ cm^{-4}$ for the InAs mode [22]. Eqs. (1) and (2) show that if L is finite, the q selection rule may relax, and additional transitions by phonon with lower energy at $q \neq 0$ may occur, which lead to the asymmetric broadening of the Raman lineshape. The dotted curves in Fig. 4 show the calculated results of the Ho-doped InGaAsP layers, which are in good agreement with experiments. From Fig. 4, the asymmetric ratio (Γ_a/Γ_b) can be evaluated from the lineshape fitting and are listed in the Table 1. It is found the asymmetric ratio (Γ_a/Γ_b) as a function of Ho amounts are almost unchanged (~1.68). This implies that the alloy disorder or the structural imperfection in InGaAsP layers is not influenced by Ho doping. The correlation lengths L, which is fitted from the calculation, are also evaluated from Fig. 4 and listed in the Table 1. It is found L values are all about 27 Å for the undoped and Ho-doped samples. Since L can be viewed as the average distance between two imperfections, the same L values also implies that no structural variance occurs after the Ho doping. What we have observed from Raman scattering suggests that the rare-earth elements do not incorporate into the LPE-grown epilayers, although they can reduce the residual impurities.

4 Conclusion

In summary, optical properties of the Ho-doped InGaAsP epilayers were studied using PL, CER, and Raman techniques. The FWHM of PL and broadening parameter of CER have been found to decrease with increasing Ho doping, indicating Ho doping greatly reduces the residual impurities and improves the quality of LPE-grown epilayers. The Raman line shapes of Ho-doped InGaAsP epilayers are asymmetric. Based on the spatial correlation model, it is found the asymmetric ratio and correlation length of the Raman signals for InGaAsP epilayers are not influenced by the Ho doping. This result suggests that no large amounts of Ho element are being incorporated into the epilayers during purification although the residual impurities can be greatly reduced.

Acknowledgement This project was supported in part by the National Science Council under the grant numbers 91-2112-M-033-012 and 92-2745-M-033-001.

References

[1] A. Cavallini, B. Fraboni, S. Pizzini, S. Binetti, S. Sanguinetti, L. Lazzarini, and G. Salviati, J. Appl. Phys. **85**, 1582 (1999).
[2] D. Seghier, T. Benyattou, A. Kalboussi, S. Moneger, G. Marrakchi, G. Guillot, B. Lambert, and A. Guivarc'h, J. Appl. Phys. **75**, 4171 (1994).
[3] M. C. Wu, E. H. Chen, T. S. Chin, and Y. K. Tu, J. Appl. Phys. **71**, 456 (1992).
[4] W. Gao, P. R. Berger, M. H. Ervin, J. Pamulapati, R. T. Lareau, and S. Schauer, J. Appl. Phys. **80**, 7094 (1996).
[5] A. Krier, H. H. Gao, and V. V. Sherstnev, J. Appl. Phys. **85**, 8419 (1999).
[6] S. Dhar, S. Paul, and V. N. Kulkarni, Appl. Phys. Lett. **76**, 1588 (2000).
[7] Y. C. Lee, H. T. Shu, J. L. Shen, K. F. Liao, and W. Y Uen, Solid State Commun. **120**, 501 (2001).
[8] V. F. Masterov and L. F. Zakharenkov, Sov. Phys. Semicond. **24**, 383 (1990).
[9] H. Nakagome, K. Takahei, and Y. Homma, J. Cryst. Growth **85**, 345 (1987).
[10] W. T. Tsang and R. A. Logan, Appl. Phys. Lett. **49**, 1686 (1986).
[11] J. P. van der Ziel, M. G. Oberg, and R. A. Logan, Appl. Phys. Lett. **50**, 1313 (1987).
[12] M. C. Wu, E. H. Chen, T. S. Chin, and Y. K. Tu, J. Appl. Phys. **71**, 456 (1992).

[13] C. M. Chiu, M. C. Wu, and C. C. Chang, Solid State Electron. **36**, 1101 (1993).
[14] O. Procházková, J. Oswald, J. Zavadil, F. Šrobár, and J. Novotný, Mater. Sci. Eng. B **44**, 160 (1997).
[15] P. Parayanthal and Fred H. Pollak, Phys. Rev. Lett. **52**, 1822 (1984).
[16] O. Procházková, J. Novotný, J. Zavadil, and K. Zdansky, Mater. Sci. Eng. B **66**, 63 (1999).
[17] M. Balkanski, Handbook on semiconductors V2 North-Holland, Amsterdam (1980).
[18] M. Balkanski, Handbook on semiconductors V2 (Completely Revised) Elsevier, Amsterdam (1994).
[19] D. E. Aspnes, Surf. Sci. **37**, 418 (1973).
[20] T. Sugiura, N. Hase, Y. Iguchi, and N. Saeaki, Jpn. J. Appl. Phys. **37**, 544 (1998).
[21] T. Sugiura, N. Hase, Y. Iguchi, and N. Saeaki, Jpn. J. Appl. Phys. **38**, 996 (1999).
[22] R. Carles, N. Saint-Cricq, J. B. Renucci, M. A. Renuui, and A. Zwick, Phys. Rev. **22**, 4804 (1980).